

Design and Control of a Reactive-Distillation Process for Glycerol Utilization to Produce Triacetin

Chung-Cheng Lee, Hao-Yeh Lee, Shih-Kai Hung and I-Lung Chien

Abstract— Due to increasing of biodiesel production in recent years, the utilization of its byproduct, glycerol, into high-value chemicals becomes more important. The esterification reaction of glycerol with acetic acid to produce triacetin is one such application. Triacetin is used mainly as a plasticizer and a gelatinizing agent in polymers, explosives and also as an additive in tobacco, pharmaceutical compounds, and cosmetics. In this study, reactive-distillation process is proposed to produce triacetin with high conversion and selectivity. Total annual cost (TAC) is minimized to obtain the optimal design flowsheet. Finally, the control strategy for this system is devised to properly reject disturbances from two feed streams

I. INTRODUCTION

The demand for renewable energy has led to an intensive research to develop industrial application of biodiesel in recent years. The output of its byproduct glycerol is also increasing. Hence, converting glycerol to high-value products has become an important issue. Triacetin is one of such products derived from glycerol. Gelosa et al. [1] used Amberlyst-15 as the catalyst in the esterification system of glycerol and the catalyst has an operating limitation under 120 °C. He proposed the reaction mechanism as a Langmuir model and verified the parameters in model by experiment data. The conventional process suffers from limited selectivity and conversion because all the three reactions are reversible. The use of reactive distillation (RD) column can be explored to obtain desire product with high selectivity and conversion. Hasabnis and Mahajani [2] used a RD column with Amberlyst-15 as catalyst and 1,2-dichloroethane (EDC) as an entrainer to remove water. Chien et al. [3] demonstrated that isobutyl acetate (IBA) is an effective entrainer to remove water in a heterogeneous azetropic column. In this paper, optimal design of a RD process is obtained by using IBA as an entrainer. Control strategy will also be developed to reject feed disturbances.

II. KINETIC AND THERMODYNAMIC MODELS

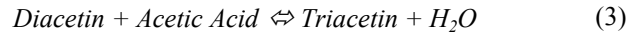
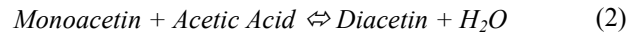
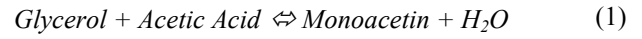
A. Kinetic Model

The three-step esterification reaction to produce triacetin is

This work was supported by the National Science Council of the R. O. C. under Grant No NSC 102-2622-E-011-020-CC1

Second author is with Department of Chemical Engineering, National Taiwan University of Science & Technology, Taipei 106, Taiwan. Other authors are with Department of Chemical Engineering, National Taiwan University, Taipei 106, Taiwan (corresponding author: I-Lung Chien, phone: 886-2-3366-3063; fax: 886-2-2362-3040; e-mail: ilungchien@ntu.edu.tw).

shown as eq. (1)-(3). There are two intermediates in the system, monoacetin (Mono) and diacetin (Diac). Both of the intermediates have two isomers. Base on the batch experiment conducted by Liao et al. [4], 1-Monoacetin and 1,3-Diacetin are chosen to represent the two intermediates respectively.



The kinetic expression of Langmuir-Hinshelwood form by using Amberlyst-15 as heterogeneous catalyst can be seen in eq. (4)-(6):

$$r_1 = k_1 \Gamma_{Gly} \Gamma_{HAc} \left[1 - \frac{\prod_{i=1}^N (\Gamma_i)^{v_{i,1}}}{K_{EQ,1}^\Gamma} \right] \quad (4)$$

$$r_2 = k_2 \Gamma_{Mono} \Gamma_{HAc} \left[1 - \frac{\prod_{i=1}^N (\Gamma_i)^{v_{i,2}}}{K_{EQ,2}^\Gamma} \right] \quad (5)$$

$$r_3 = k_3 \Gamma_{Diac} \Gamma_{HAc} \left[1 - \frac{\prod_{i=1}^N (\Gamma_i)^{v_{i,3}}}{K_{EQ,3}^\Gamma} \right] \quad (6)$$

The concentration of adsorption phase was used to calculate the reactor rate. The rates constants, concentrations, and equilibrium constants were calculated by eq. (7)-(9).

$$k_m = k_{m,0} \exp\left(\frac{-E_{A,m}}{RT}\right) \quad (7)$$

$$\Gamma_i = k_{m,0} \frac{K_i \Gamma_i^\infty C_i^L}{1 + \sum_{i=1}^N K_i C_i^L} \quad (8)$$

$$K_{EQ,m}^\Gamma = \frac{k_m}{k_{-m}} \quad (9)$$

where r_m is reaction rate (kmol/(kg-s)), k_m is forward reaction rate constant (kg/(kmol-s)), k_{-m} is backward reaction rate constant (kg/(kmol-s)), $k_{m,0}$ is pre-exponential factor, $E_{A,m}$ is activation energy of the reactions (kJ/kmol), Γ_i is the concentration of adsorption phase (kmol/kg), $v_{i,m}$ is stoichiometry coefficient, $K_{EQ,m}^\Gamma$ is equilibrium constant, T is temperature (K), R is ideal gas constant (kJ/(kmol-K)), C_i^L is

TABLE 1 Value of Parameters in Langmuir Adsorption Isotherm [1]

Species	K_i	Γ_i^∞
	m ³ /kmol	kmol/kg
Glycerol	0.714	0.00532
Acetic Acid	0.564	0.00422
Water	0.965	0.0221
Monoacetin	0.512	0.00395
Diacetin	0.310	0.00257
Triacetin	0.107	0.0012

TABLE 2 Values of Exponential Factor and Activation Energy

Reactions (m)	$E_{A,m}$	$k_{m,0}$
	kJ/kmol	kg/kmol-s
1. Gly + HAc → Mono + H ₂ O	1.46x10 ⁵	3.14x10 ²⁵
2. Mono + HAC → Diac + H ₂ O	4.07x10 ⁴	1.06x10 ⁹
3. Diac + Hac → Tri + H ₂ O	4.24x10 ⁴	6.85x10 ⁸
4. Mono + H ₂ O → Gly + HAc	1.48x10 ⁵	2.89x10 ²⁴
5. Diac + H ₂ O → Mono + HAc	2.92x10 ⁵	7.61x10 ⁶
6. Tri + H ₂ O → Diac + HAc	9.46x10 ³	7.63x10 ⁴

concentration of component i in liquid phase (kmol/m³), K_i is adsorption constant for component i (m³/kmol), Γ_i^∞ is standard constant of component i (kmol/kg). Subscript m refers to the number reaction.

B. Thermodynamic Model

There are six components in the esterification reaction with two additional entrainers (IBA and EDC) in the whole process. Glycerol and acetic acid with 95mol. % purity are fed into the system. Hasabnis and Mahajani [2] chose UNIQUAC thermodynamic model to describe the vapor-liquid and vapor-liquid-liquid equilibria. In this study, we further use Hayden-O'Connell method to more properly describe the vapor behavior of acetic acid. The binary parameters of Gly-H₂O, HAc-H₂O, HAc-IBA, H₂O-IBA use Aspen Plus built-in data with the remaining ones estimated by UNIFAC method. Table 3 shows the boiling-point and azeotropic temperature ranking of system without entrainer. Because the deactivation temperature of the catalyst is 120°C,

TABLE 3 Boling Point and Azeotropic Temperature Ranking at 0.15Bar

species	Computed Data			
	Temp. (°C)	species	Temp. (°C)	Composition (Mole basis)
H ₂ O	53.97	Diacetin	231.68	
Acetic Acid	65.21	Glycerol/ Monoacetin	224.73	0.8089/ 0.1911
Triacetin	195.32	Glycerol/ Diacetin	222.77	0.7114/ 0.2886
Glycerol	224.96	Glycerol/ Triacetin	195.21	0.0686/ 0.9314
Monoacetin	227.57	Monoacetin/ Diacetin	227.56	0.9473/ 0.0527

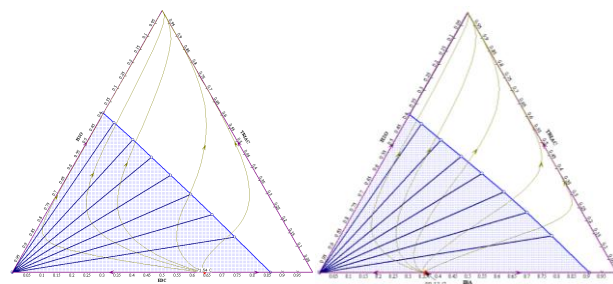


Figure 1. RCM and LLE at 40 °C of the both systems

azeotropic temperature ranking of system without entrainer. Because the deactivation temperature of the catalyst is 120°C, the operation pressure was designed for all reaction zones under this limit. The heaviest component is diacetin while the lightest component is water. However, water and acetic acid are not easy to separate. Hence, the idea of adding an entrainer to carry out water was considered.

Fig. 1 shows the residue curve map (RCM) and LLE for IBA-water-triacetin system and EDC-water-triacetin system at 1 bar. The heaviest component is triacetin, and the lightest component is the azeotropes formed by water-EDC and water-IBA with temperature of 71.54 °C and 88.13 °C respectively. Both the azeotropes can be separated into two phase naturally after cooling down to 40 °C in decanter. The organic phase stream is fed back to RD column and the aqueous phase stream is drawn out of the system.

III. OPTIMAL DESIGN FLOWSHEET

In this part, two kinds of configurations will be investigated for this process. One is for a RD column without entrainer. The other design configuration is with entrainer which has an additional decanter at the RD top (Fig. 3).

A. Reactive-Distillation Process without Entrainer

The RD system is composed mainly by three parts, rectifying, reactive, and stripping sections. The stripping

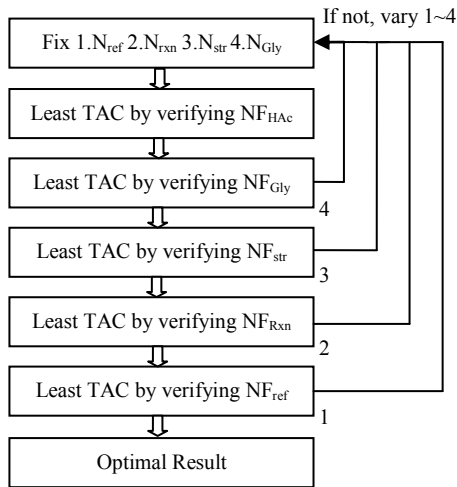


Figure 2. The optimal design flowsheet

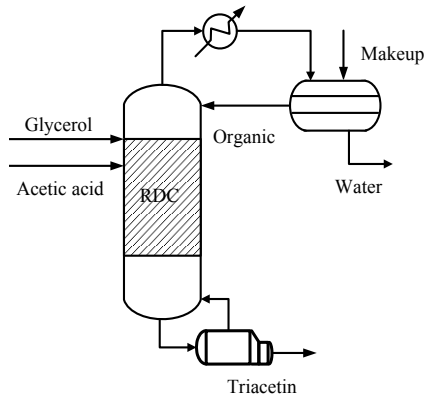


Figure 3. Proposed flowsheet of RD column with entrainer

section prevents the reaction temperature over the deactivation temperature and enhances the purity of bottom product. The rectifying section enhances the purity of top product. Top vapor of the RD column, after condensation, is partially fed back to the system. There are two design specifications for the RD column. The purity of top product is at very small acetic acid loss (0.01 mol. %) and the purity of bottom product is set to be 99 mol. % triacetin.

The design variables includes: numbers of stages of the rectifying section (N_{ref}), the reactive section (N_{rxn}), and the stripping section (N_{str}); the feed locations of glycerol (NF_{gly}) and acetic acid feed (NF_{HAc}). All these variables will be decided by TAC (total annual cost). The TAC calculation is based on Douglas [5]. We varied all the design variables step by step to get the least TAC value which is shown by Fig.2.

TAC is the sum of the operating cost and the annual capital cost. The operating cost includes steam for the reboiler, cooling water for the condenser, and catalyst cost. The capital cost includes the column shell, internal trays, reboiler, and condenser. The payback period is assumed to be 3 years in the calculation.

$$TAC = TAC_{operating} + \frac{TAC_{capital}}{3} \quad (10)$$

In the rigorous Aspen Plus® simulation of the RD column,

vapor-liquid-liquid equilibrium is allowed in each tray. The catalyst is assumed to occupy half of the holdup at each tray in the reactive section. The glycerol and acetic acid feed flow rate are set as 5 kmol/h and 15 kmol/h, respectively. Both feeds include 5 mol% of water impurity. The optimal design flowsheet will be determined by comparing the TAC of each case.

B. Entrainer-based RD

The use of entrainer decreases the boil point and keeps the reactive zone temperature below the thermal stability limit of the catalyst. Moreover, the use of entrainer also helps in increasing the efficiency of water removal. The major difference between these two configurations is additional decanter used at the top of RD column. The top vapor is not directly partially reflux to the RD column after it's cooled. It's first condensed at 40 °C and fed into a decanter to separate into two liquid phases. The organic phase is completely recycled back to top of the RD column, and the aqueous phase is drawn out of the system. Makeup flow is fed into decanter to balance the minor loss of entrainer through two outlet streams. There are two design degree-of-freedom (DOF) for this configuration. One is reboiler duty and the other one is the makeup flowrate. Reboiler duty is set to keep triacetin purity at 99 mol. % and makeup flow is set to keep top acetic acid loss at 0.01 mol. %.

The case of using IBA as entrainer is considered first. The optimal design variables of this flowsheet were obtained by the same way as in the previous subsection. Notice that the feed rates and the purity of the products are set to be exactly the same as in the previous subsection. Another case, which uses EDC as entrainer, is conducted under the same design variables as in the IBA case.

C. Comparison of the design flowsheets

The liquid flow data is shown in Table 4. As we can see in the table, the yield of the top and bottom products are almost the same. However, the organic reflux for EDC case turn out to be 330.0kmol/h. It's much larger than the value of IBA case. Although the boiling point of water-EDC azeotrope is quite low, the azeotropic composition is more water than water-IBA (see Fig. 1). This means that IBA is much more capable of carrying water to the top of the RD column. Simulation results showed that both the energy and the equipment costs of the EDC case are much more than the case of using IBA. Consequently, IBA is a better entrainer for water removal in this process. The comparisons of the optimal design flowsheet without entrainer with that of using IBA as entrainer are shown in Table 5. Notice that the trays are counting from top to bottom with the 1st tray as the condenser (or the decanter) and the last tray as the reboiler. The total number of stages of the RD without entrainer is much larger, and the reaction section is also much larger than the case with IBA as entrainer. The entrainer-based RD design can save about 19% energy requirement, but the

TABLE 4 Liquid Flow of the Two Different Entrainer

Entrainer	IBA	EDC
Liquid Flow	Flowrate (kmol/h)	Flowrate (kmol/h)
Water	15.253	15.267
Triacetin	4.776	4.785
Organic	11.586	330.0
Makeup	0.02922	0.05170

TABLE 5 Comparison of the Two Design Flowsheet

Column Configuration	Without entrainer	IBA
Total No. of trays	47	11
No. of trays in rectifying section (N_r)	9	1
No. of trays in reaction section (N_{rn})	35	7
No. of trays in stripping section (N_s)	1	1
Reactive trays	11-45	3-9
Glycerol feed tray	2	3
Acetic acid feed tray	27	4
Column diameter (m)	0.660	0.602
Reboiler duty (kW)	436.11	327.90
Total capital cost (\$1000/yr)	247.55	121.74
Column	309.05	83.37
Column trays	39.90	7.65
Heat exchangers	393.696	245.55
Decanter	-	28.65
Total operating cost (\$1000/yr)	132.49	132.77
catalyst	25.42	4.32
Energy	107.07	86.80
Makeup	-	41.65
Total annual cost (\$1000/yr)	380.04	254.51

overall operating cost is slightly higher due to the makeup cost. The total annual cost of the entrainer-based RD designs is 33% less than the RD without entrainer. From the view of the operating cost, the use of entrainer does not give an obvious benefit. However, significant total annual cost can be saved by using this entrainer-based design.

IV. CONTROL STRATEGY DEVELOPMENT

The overall control strategy of this system is developed to hold the product purity specifications under feed flow rate and feed composition changes. Pressure-driven simulation in Aspen Plus DynamicsTM is used in the control strategy development. Twenty minutes of residence time with 50% liquid level is used to calculate the volume of RD column base. The residence time of the decanter is assumed at thirty minutes in order to settle the two liquid phases.

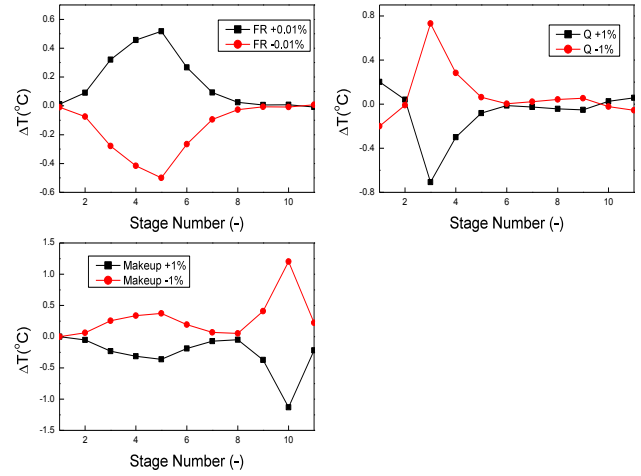


Figure 4. Open-loop sensitivity tests

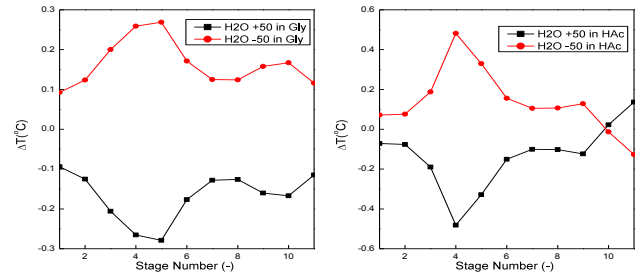


Figure 5. Closed-loop sensitivity tests

A. Inventory Control Loops

The inventory and some simple regulatory control loops are determined first. Bottom sump level is controlled by manipulating the triacetin product flow. The organic phase level in the decanter is controlled by the organic reflux flow. The aqueous phase level is controlled by the aqueous outlet. Top pressure of the RD column is assumed to be controlled by the top overhead vapor flow rate. In real industrial situation, the operating pressure which is less than atmospheric pressure can be maintained by a vacuum system. The decanter temperature is controlled at 40 °C by the cooler duty. A ratio scheme for determining the acetic acid feed flow is implemented to maintain a constant feed ratio, while the value of this constant can be manipulated by a tray temperature control loop.

After the inventory control loops are determined, there are three manipulated variables left. They are: feed ratio, reboiler duty, and the makeup flow rate. These three manipulated variables can be used to hold the product purities in spite of feed disturbances.

B. Tray Temperature Control Loop(s)

It is assumed that the online composition measurement is either unavailable or may maintain troublesome, thus tray temperature(s) will be used to indirectly hold the product specifications. The simplest overall control strategy is to consider single tray temperature control loop. In this case, if

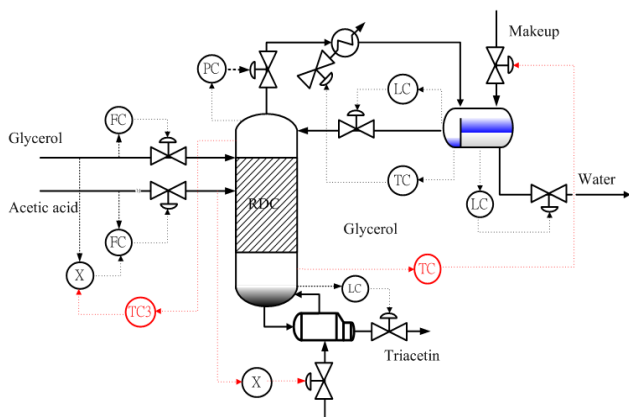


Figure 6. Overall control strategy of the proposed design.

only one of the remaining variables is selected as the manipulated variable for the temperature control loop, the feed ratio should be selected. The reason is that maintaining of the correct stoichiometric ratio of the two reactants is crucial for a RD column, otherwise the un-reacted reactant would be a waste. Because the feed composition disturbances are assumed to be unmeasured, the acetic acid/glycerol feed ratio needs to be adjusted via the tray temperature loop in order to hold at the correct stoichiometric ratio. For single temperature control strategy, the other two design variables are often maintained at some ratio to other variables in the system.

For this design, it is not possible to use the simplest single-loop control strategy. The problem was mainly due to the unmeasured feed composition variations inevitably occurred in the system. It turns out that besides the feed ratio, at least one of the remaining design variables needs to be adjusted by another tray temperature control loop.

One important question is which one should we select as the second manipulated variable? The answer of this question can easily be obtained by open-loop and closed-loop sensitivity of the system. With the information of both sensitivity tests (Fig. 4 and 6), the upper stages shows significant sensitivity to the feed ratio and the bottom stages are sensitive to makeup flowrate. Hence, the makeup flowrate is selected as the second manipulated variable instead of reboiler duty.

From the two figures of sensitivity tests, stage 3 and stage 10 were chosen for the temperature control. Obviously, stage 10 temperature has the most deviation when makeup flowrate changes and least deviation for closed-loop sensitivity test. For another controlled variable, there is a trade-off for the determination of control point. Although stage 5 temperature has the most deviation in the open-loop sensitivity test, it also has the same situation in the closed-loop sensitivity test. As a result, we choose stage 3 for its best response of the disturbance. The remaining manipulated variable need to be determined is the reboiler duty. From closed-loop sensitivity tests, all operating variables of the system at desired values can be determined to perfectly control two product purities under unmeasured feed composition disturbances.

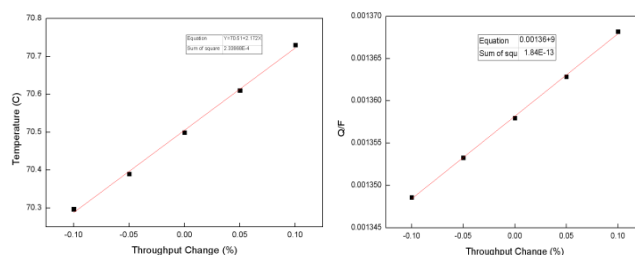


Figure 7. Relation between setpoint and throughput changes

By observing the candidate ratios with the reboiler duty, fixing the ratio of reboiler duty/acetic acid feed at a constant value is selected. The proposed overall control strategy is summarized in Fig. 6.

All level loops were tuned using P-only controller with $K_c=2.0$ except for the organic level loop using $K_c=10.0$ to speed up the response of the recycle loop. Tight PI tuning constants was chosen for the pressure control loop. The remaining two crucial tray temperature loops were tuned using iterative relay-feedback tests with Tyreus-Luyben [6] tuning rules until the tuning constants were converged.

C. Closed-Loop Disturbance Rejection Tests

Two disturbance rejection tests were introduced to observe the controllability and operability of the control strategy. The first test is to allow for throughput changes. These can be done by increase/decrease the setpoint of the glycerol feed flow loop. Because the throughput changes are considered as a known disturbance, we could change both the setpoints of tray temperature and Q/F ratio in order to maintain the purity of the products. The tray temperatures mainly effect the extent of reaction and the reboiler duty influences the separation of HAc and water, and there are linear relations between the percentage of throughput changes and setpoint value (Shown in Fig. 7). The setpoint of stage 10 temperature control loop needs not to be changed under throughput changes. Fig. 8 displays the closed-loop results with up to +10% and down to -10% throughput changes for the proposed control strategy. The two controlled tray temperatures are all returned back to their setpoints (See two middle column plots in Fig. 8.). By observing the manipulated variable of the stage 3 temperature loop, the feed ratio also returned back to the correct stoichiometric ratio after some transient responses. The changes of the makeup flow rate is dictated by the temperature control loop of stage 10, while the reboiler duty is correspondingly increased /decreased by a ratio scheme in the control strategy in Fig. 7. The major test is the purity of the two main products, glycerol and water. It is observed that the two purities can be controlled back to the original specifications (see two top plots in Fig. 8) after varying the setpoint of one temperature control loop and the Q/F ratio. The next disturbance test is the feed composition changes. This is a very realistic situation because the inert (water) in this glycerol feed often varies. Fig. 9 displays the closed-loop responses with up to +50% and down to -50% changes of the water content in this feed stream. The control strategy needs to adjust the feed ratio downward when there is more inert in

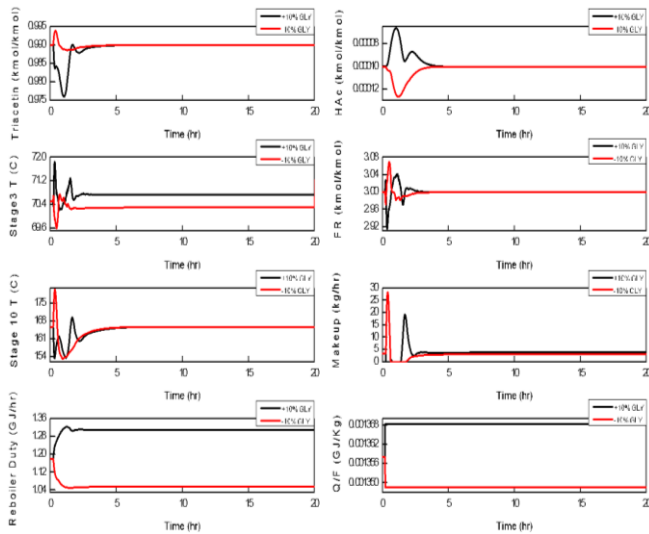


Figure 8. Response of throughput changes

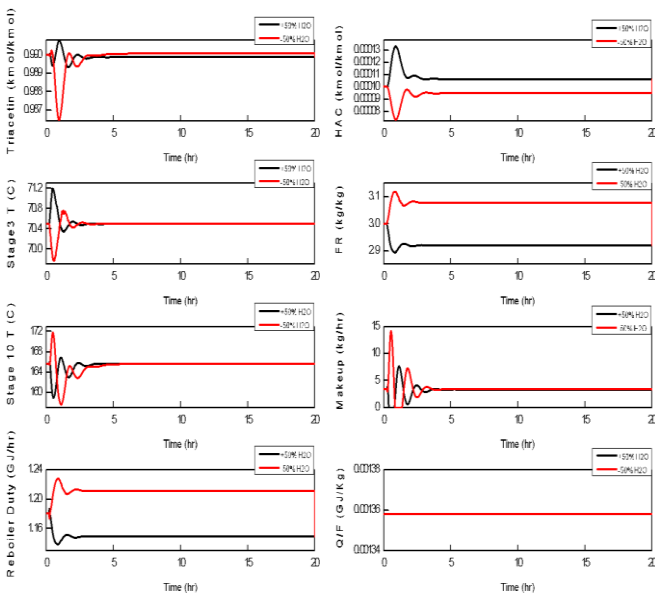


Figure 9. Response of feed composition changes

this feed stream so that the stoichiometric ratio can still be maintained between glycerol and acetic acid.

From the closed-loop results, it is observed that the control strategy fulfill its goal in correctly adjusting the feed ratio during feed composition changes. The purity of the triacetin product has only a small deviation from the design values. The rejection of feed composition disturbance in acetic acid is also simulated with up to +50% and down to -50% changes of the water content. The purity of triacetin is about 0.991 and 0.989 mol% under the two disturbances. Due to page limit, dynamic responses with HAc feed composition changes are not shown.

V. CONCLUSION

This study presents a feasible design for the esterification of glycerol with acetic acid. Three design flowsheets are explored in this work: one RD process without entrainer and

two entrainer-based RD processes. The best process is determined based on TAC savings. By comparison, it is shown that entrainer-based RD using IBA as entrainer is the best design flowsheet with significant least TAC than the other two designs.

The overall control strategy of the proposed design flowsheet is also determined. Two tray temperatures (stages 3 and 10) in the RD column are controlled by manipulating feed ratio and makeup flow rate. The remaining manipulated variable of reboiler duty is maintained at a constant ratio to HAc feed. From the dynamic disturbance rejection tests, the proposed design is capable of holding product specifications despite throughput and feed composition changes.

REFERENCES

- [1] D. Gelosa, M. Ramaioli, G. Valente, and M. Morbidelli, "Chromato-graphic reactors: Esterification of glycerol with acetic acid using acidic polymeric resins," *Ind. Eng. Chem. Res.*, vol. 42, pp. 6536–6544, 2003.
- [2] A. Hasabnis and S. Mahajani, "Entrainer-based reactive distillation for esterification of glycerol with acetic acid," *Ind. Eng. Chem. Res.*, vol. 49, pp. 9058–9067, 2010.
- [3] I. L. Chien, K. L. Zeng, H. Y. Chao, and J. H. Liu, "Design and control of acetic acid dehydration system via heterogeneous azeotropic distillation," *Chem. Eng. Sci.*, vol. 58, pp. 4547–4567, 2004.
- [4] X. Liao, Y. Zhu, S. G. Wang, H. Chen, and Y. Li, "Theoretical elucidation of acetylating glycerol with acetic acid and acetic anhydride," *Appl. Catal. B.*, vol. 94, pp. 64–70, 2010.
- [5] J. M. Douglas, *Conceptual Design of Chemical Processes*. New York: McGraw-Hill, 1988.
- [6] W. L. Luyben and M. L. Luyben, *Essentials of Process Control*, New York: McGraw-Hill, 1997, pp. 97–98.